ADVANCED FUNCTIONAL MATERIALS
www.afm-journal.de

Triplet–Triplet Annihilation-Based Anti-Stokes Oxygen Sensing Materials with a Very Broad Dynamic Range

Sergey M. Borisov, Christoph Larndorfer, and Ingo Klimant*

A novel concept for designing optical oxygen sensing materials is reported. Oxygen-sensitive anti-Stokes emission is generated via triplet–triplet annihilation-based upconversion and serves as an analytical parameter. Porous glass beads are used to incorporate the "sensing chemistry" including a sensitizer and an annihilator dissolved in a high boiling solvent. The beads are dispersed in silicone rubber or Teflon AF to produce solid state optodes. Inexpensive low power light sources (LEDs) are used for the excitation. The upconverted emission shows unmatched sensitivity both for the luminescence decay time and for the luminescence intensity. The latter features unusual quadratic Stern-Volmer plots. Much lower sensitivity of the residual NIR luminescence of the sensitizer allows determination of pO_2 in the broad dynamic range from trace oxygen quantities to ≈40 kPa. Interrogation of the sensors in frequency domain is demonstrated. Influence of the excitation light power on the calibration, temperature effects, dynamic response to altering pO_2, and photostability of the sensing materials are also investigated.

1. Introduction

Optical oxygen sensors became increasingly popular in the last decades. These analytical tools are now routinely used in biological, medical, biotechnological and marine studies, but also in numerous industrial applications; they represent a promising alternative to the Clark's electrode.[1–4] Recent years have seen much progress in the field of oxygen indicators where many new dyes with improved properties (luminescence brightness,[5] photostability,[6] long-wave excitation and emission) were introduced. Particularly, NIR emitting indicators gained increasing significance[7–14] due to the fact that they enable oxygen monitoring in various biological samples and in tissues where conventional UV-Vis indicators fail because of high scattering and low penetration depth of the visible light. Moreover, excitation in the red or NIR part of the spectrum usually results in much lower levels of autofluorescence. Samples containing photosynthetic pigments absorbing in the red part of the spectrum represent a notable exception.

Another exciting possibility to completely eliminate background fluorescence is to use anti-Stokes oxygen-sensing materials. In theory, such non linear optical materials may also improve spatial resolution in imaging applications since the emission intensity is not directly proportional to the excitation intensity. Consequently, the signal cross-talk from other areas (where the excitation intensity is lower) can be minimized. However, only a few anti-Stokes sensing materials (including optical oxygen sensors) have been reported so far and this field still remains in its infancy. Particularly, Vinogradov and co-workers reported several two-photon-excitable oxygen-sensitive dendrimeric probes and demonstrated their application for imaging in tissues.[15–17] Doubtlessly, these probes represent very valuable analytical tools but they are mostly limited to microscopic imaging. In fact, multiphoton excitation is only possible under very high energies of the excitation light and the respective instrumentation (e.g., Ti-sapphire laser) is not inexpensive. As an alternative, Wolfbeis and co-workers reported a completely different type of anti-Stokes sensing materials. Lanthanide phosphor nanoparticles (known to exhibit upconverting luminescence under moderately intense NIR excitation) were used as "nanolamps" to excite a luminescent indicator. The authors demonstrated feasibility of the approach for designing oxygen,[18] pH,[19] carbon dioxide[20] and ammonia sensors[21] although the signal to noise ratio was rather low in certain cases.

Triplet-triplet annihilation (TTA)-based upconversion represents yet another possibility to obtain anti-Stokes fluorescence. Although being known for several decades, TTA-based upconversion recently became of much interest due to potential applications in photovoltaics and photocatalysis. In fact numerous solution-based systems have been reported in last decade.[22–36] Such systems include a sensitizer (typically a metal-ligand complex having high quantum yield of triplet state formation) and an annihilator (usually a polycyclic aromatic hydrocarbon with the triplet state located lower than that of the sensitizer) dissolved in an organic solvent. Thus, the annihilator in the triplet state can be accumulated upon excitation of the sensitizer due to efficient triplet-triplet energy transfer from the sensitizer to the annihilator. The upconverted fluorescence is produced by the annihilator molecules in the singlet state generated during the triplet-triplet annihilation. Although TTA-based upconverting systems were demonstrated to be rather efficient in solutions of organic solvents, the attempts to design solid state compositions based on polymeric materials were less successful. Much

Dr. S. M. Borisov, C. Larndorfer, Prof. I. Klimant
Institute of Analytical Chemistry and Food Chemistry
Graz University of Technology
Stremayrgasse 9, 8010, Graz, Austria
E-mail: sergey.borisov@tugraz.at

DOI: 10.1002/adfm.201200794

lower efficiency of upconverting fluorescence in polymeric films[37,38] is explained by high viscosity of the polymer matrices which results in limited molecular mobility and strongly reduced interaction probability of the components.[38,39] This can be partly overcome by using rubbery polymeric materials[40] but the emission intensity at room temperature remains quite low.[41] A recent report demonstrated efficient upconversion in polystyrene nanoparticles.[39]

We perceived that it is possible to design optical oxygen sensors which will employ TTA upconversion since triplet states are known to be efficiently quenched by molecular oxygen. This paper will show how to realize a solid state optical oxygen sensor based on the above principle. We will demonstrate the unique properties of the system which apart from the upconversion capability include the possibility of ratiometric and lifetime sensing and the suitability for sensing in a very broad dynamic range not achievable with conventional oxygen sensors.

2. Results and Discussion

2.1. Sensing Mechanism

State-of-the-art optical oxygen sensors rely on quenching of luminescent molecules by molecular oxygen. Due to relatively long lifetime of the excited triplets (μs-ms) oxygen quenching is the most efficient for the complexes of Pd(II), Pt(II), Ir(III), Cu(I), Ru(II) etc. In these complexes the triplet state is populated with probability close to unity due to the heavy atom effect. Typical indicator classes include complexes of porphyrins, polypyridyls and cyclometallating ligands but many other systems have been reported. On the other hand, these or similar metal complexes can act as sensitizers in TTA-based upconversion systems. Evidently, an optical oxygen sensor with upconverting capability can be designed. The Jablonsky diagram (**Figure 1**) provides an overview of the processes which occur in such a sensor. Briefly, a sensitizer is promoted to the excited singlet state during the excitation. Due to efficient inter-system crossing (ISC) the triplet state of the sensitizer becomes populated. The annihilator in the triplet state is produced via triplet-triplet energy transfer (TT ET). Finally, annihilation of these triplets gives annihilator in the singlet excited state which emits anti-Stokes fluorescence. Both triplets of the sensitizer and the annihilator can be quenched by molecular oxygen. A more detailed summary of the processes which occur in a TT-upconversion based oxygen sensor can be found in Figure S1 (Supporting Information). Apart from the above mentioned processes these include radiative and radiationless deactivation of the sensitizer and annihilator in the singlet and in the triplet excited state.

2.2. Choice of Materials

A variety of sensitizers and annihilators were reported to perform well in TTA upconversion systems. These include, for example, Ru(II) polypyridyls,[30,42] Pt(II) and Pd(II) complexes with porphyrins[28,23,32,39–41] and phthalocyanines,[22,43] cyclometallated Pt(II) complexes,[25] supramolecular chromophores[44] as sensitizers and rubrene,[22] perylenes,[32,44] anthracenes,[30,39,42] borodipyrroles[23] as annihilators. In principle, virtually all reported combinations can be used to design an oxygen sensor. However, it should be considered that good compatibility of the indicators with the excitation sources is essential for optical sensors. Therefore, Pt(II) and Pd(II) complexes with tetraphenyltetrabenzoporphyrin (TPTBP, Figure 1) were sensitizers of choice since they enable excitation with the red light and are compatible with 605 and 625 nm LEDs. PdTPTBP can be also excited with a 635 nm laser diode or a He-Ne laser, however excitation of PtTPTBP with these light sources is less efficient. A perylene dye diisobutyl 3,9-perylenedicarboxylate (known as Solvent Green 5, Figure 1) was used as annihilator. This dye possesses good solubility in most organic solvents and similarly to other perylene dyes was expected to have excellent photostability.[45] Importantly, the fluorescence maximum of the perylene is at ~505 nm where the absorption of the benzoporphyrin complexes is inefficient; this is expected to minimize potential Föster resonance energy transfer (FRET) from the perylene in the singlet excited state to the porphyrin.

2.3. Sensor Design

As was mentioned above, strong upconverted fluorescence was reported for numerous solution-based systems, but the process

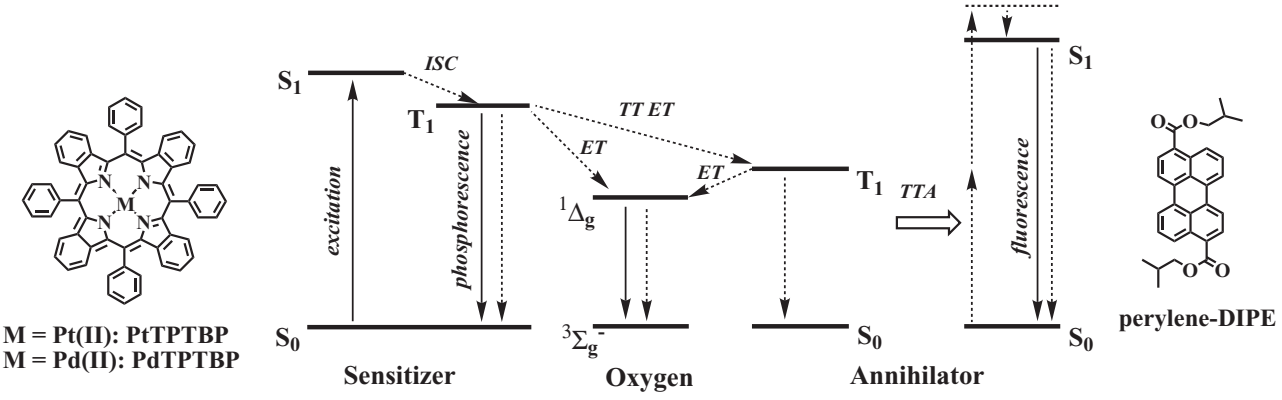

Figure 1. Simplified Jablonski diagram illustrating the mechanism of the TTA-based upconversion and quenching of the excited species by molecular oxygen. The chemical structures of the sensitizers (left) and of the annihilator (right) are also shown.

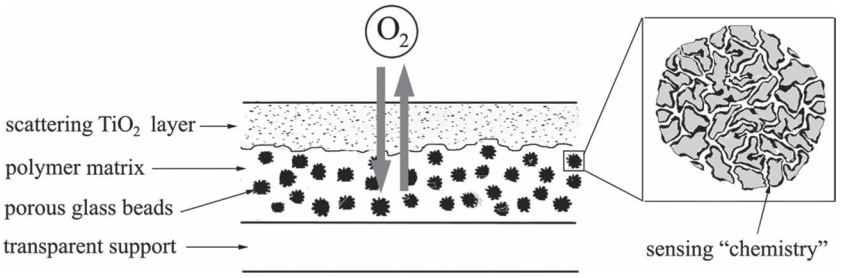

Figure 2. Cross-section of the oxygen sensor.

was much less efficient in rigid polymeric matrices. Even in rubbery polymers the upconversion efficiency was found to be rather low at room temperature but significantly improved at higher temperatures.[37] Temperatures of 0–40 °C are relevant for most oxygen sensing applications; therefore, the above materials seem to be not adequate for designing a bright TTA-based oxygen sensor operating in this temperature range. Our preliminary experiments indicated that the upconversion efficiency was virtually negligible in a such non rigid matrix as plasticized poly(vinyl chloride). Provided here is an elegant solution for the oxygen-sensing material which combines the mechanical properties of the solid-state sensor but simultaneously preserves the solution-based chemistry of a conventional upconversion system. **Figure 2** schematically illustrates the composition of the planar optical sensor. The sensitizer PtTPTBP or PdTPTBP (C = 0.9 or 1.1 mM, respectively) and the annihilator Solvent Green 5 (2.2 mM) are dissolved in an organic solvent, e.g., in a common plasticizer n-butyl benzyl phthalate (BBP). The high boiling point of the solvent (370 °C for BBP) is important to prevent evaporation. Alternatively, poly(propylene glycol) (PPG, vapor pressure < 0.01 mm Hg at 20 °C) was found to be a suitable solvent. Then, porous glass microparticles are soaked with this solution which is distributed within the pores of the beads. Thus, liquid phase is preserved inside the microparticles. The microparticles are dispersed in an inert polymer matrix and the sensing composition is coated on a transparent support (poly(ethylene terephthalate) or glass). Silicone rubber (prepared by cross-linking the silicone primers) and Teflon AF 1600 were found to be suitable matrices since the following requirements are fulfilled: a, the materials are highly permeable to oxygen; b, both polymers are extremely bad solvents for the dyes and the liquid polymers so that no extraction can occur; c, dilution of the polymers with certain organic solvents (hexane and perfluorodecalin for the silicone and Teflon AF, respectively) can be done for convenient processing of the sensing materials, and these solvents do not interfere with the sensing chemistries of the particles. The thickness of the sensing layer was about 35 μm for the silicon rubber (containing 35% w/w of the beads) and about 11 μm for the Teflon AF composition (containing 66% w/w of the beads). It should be noted here that the polymer not only acts as a support for the particles but also as a permeation-selective membrane which protects the "sensing chemistry" from interferences. Indeed, both polymers are highly hydrophobic and are not permeable for ionic species but are highly permeable for gases including oxygen. This makes it possible for the sensor to operate both in the gas phase and in aqueous solutions. An additional scattering layer (containing TiO_2 nanobeads dispersed in silicone rubber or Teflon AF) was coated above the sensing layer. The scattering layer enhances the signals of the sensor by increasing the optical path of the excitation light and because of better outcoupling of the emission light.[46] **Table 1** provides an overview of the sensing materials investigated.

2.4. Optical Properties

Figure 3 shows the photographic images of a cuvette with a sensing foil (PdTPTBP, BBP in silicone) excited with the red light from high power 635 nm LED. As can be seen, the sensing material is capable of generating bright green fluorescence in the absence of oxygen. It should be noted that conventional 5 mm LEDs can be also used to efficiently generate upconverted fluorescence even in combination with an optical fiber. Thus, the realization of a fiber-optic sensor was made possible.

Figure 4 shows the corrected emission spectra of sensing material SM1 upon excitation in the Q-band of the Pt(II)-benzoporphyrin. Both the anti-Stokes green fluorescence from the perylene dye (λ_{max} = 505 nm) and the phosphorescence from the benzoporphyrin (λ_{max} = 770 nm) are observed. The quantum yield of the upconverted fluorescence was estimated by comparison of the emission of the perylene and the residual phosphorescence of PtTPTBP. It was assumed that the quantum yield for PtTPTBP is proportional to its decay time (5.9 μs), i.e., is 5.9% in the sensing material (compare to the quantum yield of 50% and the decay time of 50 μs in deoxygenated toluene). The quantum yield of the upconverted fluorescence for the sensor SM1 at the photon flux density of 240 μmol s^{-1} m^{-2} was estimated to be about 2% which is significantly lower that the calculated theoretical limit of a typical upconversion system of about 25%[43] (achieved only at high light intensities). On the other hand, this value is more than sufficient to obtain high S/N ratios. Notably, this condition is fulfilled even at significantly lower emission intensities since the background signal (typically generated by fluorescence of the optical components such as fibers and filters, autofluorescence of the probe, etc.) is virtually absent. Due to this fact the materials can be promising for application in media with high level of background fluorescence (e.g., photosynthetic systems). Although the background fluorescence can be easily eliminated in time domain measurements (by using a short time delay) it usually strongly affects

Table 1. Composition of the oxygen sensing materials.

Sensor code	Sensitizer	Organic solvent	Polymer matrix
SM1	PtTPTBP	BBP	Silicone rubber
SM2	PtTPTBP	PPG	Silicone rubber
SM3	PtTPTBP	PPG	Teflon AF 1600
SM4	PdTPTBP	BBP	Silicone rubber

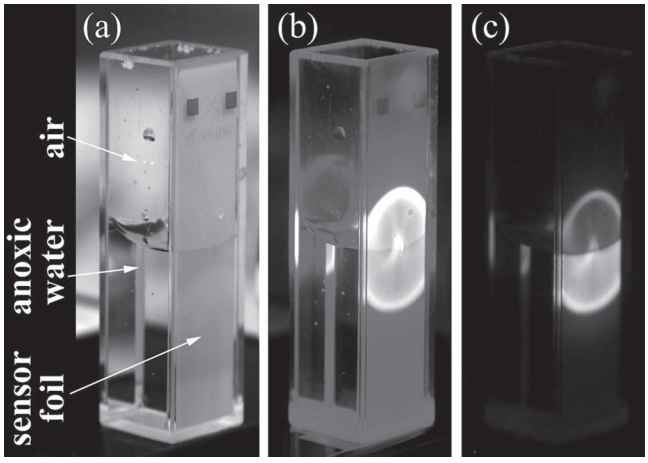

Figure 3. Photographic images of a glass cuvette containing a sensing foil (SM4 on poly(ethylene terephthalate) support) and deoxygenated water. a) Daylight photo without excitation. b,c) Dark images obtained under excitation with a 635 nm 3 W LED. In case of (c) a plastic band-pass filter ("Peacock Blue" from Lee Filters) was used in front of the camera.

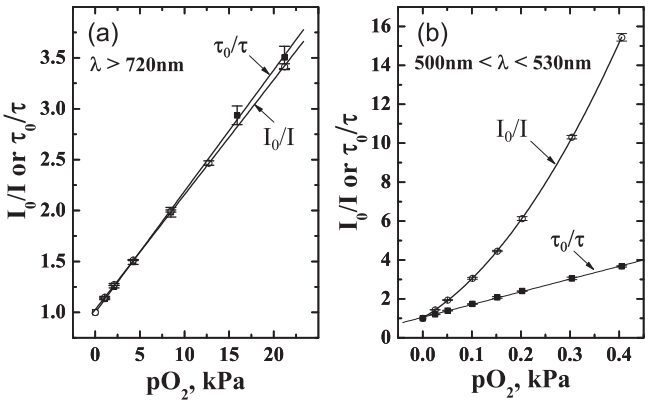

Figure 5. Stern-Volmer plots for the oxygen sensor SM1 excited with a 605 nm LED and monitored using an RG 9 long-pass filter at a modulation frequency of 30 kHz (a) and using a 515/30 band-pass filter at a modulation frequency of 555 Hz (b). Linear fit was used for all the dependencies except for the intensity dependence of the upconverted fluorescence which was fitted using a quadratic equation.

the frequency domain measurements and ratiometric luminescence intensity measurements.

The excitation spectra for the sensors SM1 and SM4 (Figure S2, Supporting Information) were recorded by monitoring the emission at 505 nm and they were found to be identical to the absorption spectra of the sensitizers PtTPTBP and PdTPTBP,[47] respectively.

2.5. Oxygen-Sensing Properties

The luminescences originating from the sensitizer and the annihilator decrease in the presence of molecular oxygen (Figure 4). Notably, the fluorescence of the perylene decreases much more significant than the NIR phosphorescence of the porphyrin. In fact, the fluorescence of the perylene dye disappears almost completely at 1 kPa O_2 and decreases to approx. 15% of the original value at 0.2 kPa O_2. On the other hand, the phosphorescence intensity of PtTPTBP at the same pO_2 is about 95% of the original value. More detailed analysis reveals that quenching of PtTPTBP can be described by a Stern-Volmer equation, where decrease in the intensity I_0/I is directly proportional to the oxygen concentration (**Figure 5**a). Notably, the Stern-Volmer plots show excellent linearity (correlation coefficient > 0.9997) and are virtually identical for both the intensity and the decay time. Such behavior is common for quenching by oxygen in solutions. It should also be noted that the decay time of PtTPTBP in the sensing material in the absence of oxygen (τ_0) is only 5.9 μs (Figure S3, Supporting Information). This is nearly one order of magnitude lower than the values obtained for the same dye in organic solvents in the absence of the annihilator (τ_0 about 50 μs) which indicates a high efficiency of the triplet-triplet energy transfer process. The triplet-triplet energy transfer appears to be even more efficient in the PdTPTBP-based sensor since the phosphorescence of the sensitizer is quenched almost completely (Figure S4, Supporting Information). Therefore, it was not possible to determine the decay times of the sensitizer.

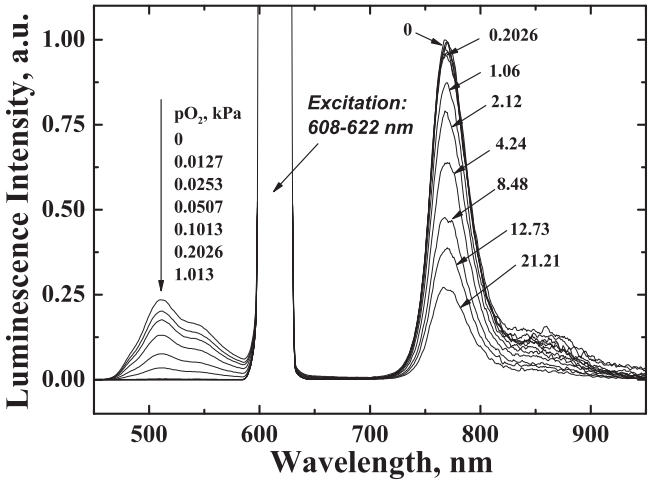

Figure 4. Emission spectra at varying pO_2 for the sensing material SM1, λ_{exc} = 615 nm, 20 °C.

The quenching behavior observed for the upconverted fluorescence is more complex than for the phosphorescence of the sensitizer. However, the luminescence decay can be adequately described using the mono-exponential model (e.g. see Figure S5, Supporting Information, for the sensor SM4). Notably, the simulation experiments (Supporting information) also predict mono-exponential decay (Figure S6, Supporting Information) for all the sensing materials if the following conditions are assumed: a) the decay time of the sensitizer is much shorter than that of the annihilator which is valid for all investigated sensors and b) the TTA process is far less likely than the radiativeless deactivation of the annihilator triplets which seems plausible at low excitation light intensities employed (240 μmol s^{-1} m^{-2}). It is also revealed that the decay times for the triplet state of the annihilator can be roughly estimated as the double of the observed decay times of the upconverted fluorescence.

Table 2. Properties of the oxygen-sensing materials at 20 °C.

Material	Upconverted fluorescence			NIR phosphorescence		
	τ_0, µs	τ_0/τ - 1 at 0.405 kPa O_2	I_0/I - 1 at 0.405 kPa O_2	τ_0, µs	τ_0/τ - 1 at 21.21 kPa O_2	I_0/I - 1 at 21.21 kPa O_2
SM1	200	2.7	14.5	5.9	2.5	2.4
SM2	260	4.1	70	21.2	9.0	8.6
SM4	240	3.2	20.0	n.d.	n.d.	n.d.

All measurements were performed in frequency domain at modulation frequencies of 555 Hz and 30 kHz for the upconverted fluorescence and the NIR phosphorescence, respectively.

Determination of the decay times in frequency domain is quite common in optical sensing since compact and cheap instrumentation can be used. In this method, the average decay times can be calculated as $\tau = \tan\Phi/2\pi f$, with Φ being the luminescence phase shift at the modulation frequency (f). The calculated decay times were found to be close to the values obtained in the time domain measurements (Figure S7, Supporting Information). Thus, the sensors can be indeed calibrated using the frequency domain set-up. Notably, the decay times are similar for the materials based on different sensitizers (**Table 2**) which is in agreement with the simulation experiments (Figure S6, Supporting Information).

Analysis of the Stern-Volmer plots for the upconverted fluorescence (Figure 5b) reveals that: a) the decay time plots are linear and the sensitivity is directly proportional to the oxygen partial pressure; b) the intensity plots are non-linear and the sensitivity increases at higher pO_2; and c) the fluorescence intensity is extremely sensitive to oxygen but the sensitivity of the decay time is also rather high. In fact, the τ_0/τ-1 values obtained for the upconverted fluorescence at 0.405 kPa are about 57-fold higher (SM1, Table 2) than for the NIR phosphorescence. The Stern-Volmer constant calculated from the decay time plot is as high as 6.6 kPa^{-1}. This is higher than the value obtained for trace oxygen sensors based on a Pt(II) porphyrin embedded in silica-gel (K_{SV} ~ 4 kPa^{-1}),[48] but is lower than for trace sensors based on a Pd(II) porphyrin in the same matrix (K_{SV} ~ 65 kPa^{-1}),[48] one of the most sensitive materials reported so far.

The non-linear Stern-Volmer dependence of the fluorescence intensity is particularly interesting since such behavior is not observed for conventional optical oxygen sensors. The Stern-Volmer curve can be best described using a quadratic function (correlation coefficient $r^2 > 0.9999$) which is in full agreement with theoretical expectations (see Supporting information for more details). In fact, the simulated curves are very close to those obtained experimentally (Figure S8, Supporting Information). Notably, the calculations also predict linear Stern-Volmer plots for the decay time of the upconverted emission with the slopes similar to the ones observed experimentally (Figure S8, right and Figure 5b, respectively).

New oxygen sensors based on TTA upconversion can be of particular interest for a number of applications in which monitoring of oxygen in a very broad dynamic range is necessary. Conventional oxygen sensors are not fully adequate here. In fact, the sensors designed for a normal range from 0 to 40 kPa O_2 do not provide adequate resolution at $pO_2 < 1$ kPa, and the trace oxygen sensors are not reliable at $pO_2 > 4$kPa since the intensity is dramatically decreased and the S/N ratio is low. The materials reported in this contribution overcome these drawbacks. Indeed, monitoring of extremely low oxygen quantities is possible via measuring luminescence intensity of the upconverted fluorescence. Measuring the luminescence intensity ratio of the upconverted fluorescence and NIR fluorescence (which remains virtually unaltered up to 0.2 kPa O_2) should yield even better results. Low oxygen concentrations can be detected by measuring luminescence decay times of the upconverted fluorescence. Finally, relatively high pO_2 (1–40 kPa) can be accessed by measuring the decay times of the NIR phosphorescence. A measurement device operating in frequency domain and containing one excitation source (an LED or a laser diode) and two photodetectors with adequate optical filters can be certainly realized. It should be mentioned here that more conventional concepts for realization of the broad dynamic range sensor are of course possible. Evidently, such a sensor can be obtained by combining two oxygen indicators with significantly different decay times e.g. platinum(II) and palladium(II) porphyrins.

2.6. Effect of the Sensor Composition on the Oxygen-Sensing Properties

Table 2 provides an overview of the sensing characteristics of the investigated materials. As can be seen, substitution of PtTPTBP by the Pd(II) complex has only a minor effect on the sensitivity which increases slightly (SM1 and SM4, respectively). On the other hand, the nature of the solvent used for the sensitizer and the annihilator is much more important. Indeed, if n-butyl benzyl phthalate (SM1) is substituted by poly(propylene glycol) (SM2) the sensitivity of the upconverted fluorescence improves by about 2-fold for the decay time and about 5-fold for the intensity. Since the decay time increases only slightly (from 200 to 260 µs); this may indicate faster diffusion or better solubility of oxygen in this solvent. Simultaneously, the decay time of PtTPTBP increases by about 4-fold. PPG may restrict the diffusion of rather large molecules of the sensitizer and the annihilator thus reducing the efficiency of T-T energy transfer. As can be seen, quenching of the NIR phosphorescence by oxygen is also more efficient in PPG compared to BBP but this can be attributed to longer decay times of PtTPTBP. Finally, the nature of the polymer matrix (silicone rubber or Teflon AF) in which

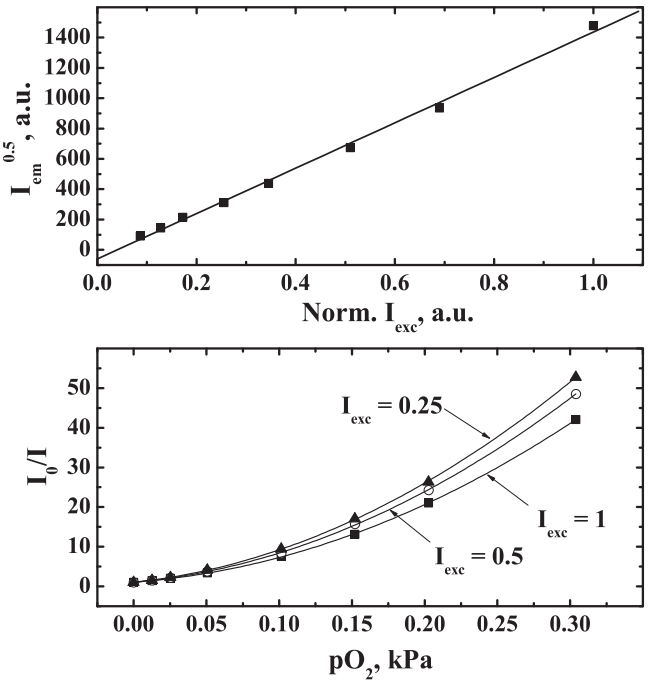

Figure 6. The effect of the excitation intensity on the intensity of the upconverted fluorescence (a) and on the sensitivity to oxygen (b) for the sensor SM2 (λ_{exc} = 615 nm, λ_{em} = 505 nm). I_{exc} = 1 corresponds to 240 μmol s^{-1} m^{-2} photons.

the beads are dispersed evidently has no influence on the sensitivity (Figure S9, Supporting Information).

2.7. Influence of the Excitation Power on Sensing Properties

As documented in the literature the emission intensity in the TTA-based upconversion systems is often proportional to the square of the excitation intensity (I_{exc}).[22,23,40,41] **Figure 6**a demonstrates that this is also valid for the optical sensors based on TTA upconversion. Such behavior is also predicted theoretically (Figure S10, Supporting Information) for relatively low light intensities. In fact, the intensity of the excitation light was estimated to be about 240 μmol s^{-1} m^{-2} (4.7 mW cm^2) in the fluorescence spectrometer set-up and about 95 μmol s^{-1} m^{-2} (1.8 mW cm^2) in the fiber-optic set-up for frequency domain experiments. At these light intensities only a small portion of the sensitizer (and annihilator) is present in the triplet excited state. Excitation of the sensor SM4 with a 635-nm red laser diode (which is spectrally compatible to the Q-band of PdTPTBP) indicates a threshold value of about 1000 μmol s^{-1} m^{-2} of photons (18.8 mW cm^2) above which deviation from the quadratic dependence is clearly visible (Figure S11, Supporting Information). For comparison, other upconverting systems in solutions were reported to obey quadratic dependence at the irradiance values up to 20 mW cm^2 [22] and 27 mW cm^2,[40] however only a linear dependence between 14.2 and 238 mW cm^2.[35]

Interestingly, the intensity of the excitation light slightly affects the Stern-Volmer plots for the intensity of the upconverted fluorescence (Figure 6b). As shown, quenching becomes more efficient at lower I_{exc}. The simulation experiments produce similar results (Figure S12, Supporting Information). The important consequence is that pronounced variation of the excitation intensity due to instability of the light source, absorption or scattering of the excitation light by optical components or the analyzed medium will result in different calibration plots for the luminescence intensity. This may limit practical applicability of the above analytical parameter since the calibration and measurements should be performed in identical light conditions. Fortunately, almost no dependence of the decay time (and the corresponding decay time Stern-Volmer plots) is predicted (Figure S13, Supporting Information) for the upconverted fluorescence. Notably, the Stern-Volmer plots for the residual NIR phosphorescence are also independent on the intensity of the excitation light (Figure S13, Supporting Information).

2.8. Temperature Influence

Temperature is known to affect the calibration of all optical oxygen sensors. For most conventional sensors (which in the simplest case consist of an oxygen indicator dissolved in a polymer) the sensitivity increases with temperature because the diffusion of the quencher becomes faster. Simultaneously, the luminescence decay times τ_0 decrease due to thermal quenching. Evidently, the situation should be more complicated for the optical sensors based on TTA upconversion since the efficiency of the triplet-triplet energy transfer is affected by temperature. Furthermore, our sensors employ the sensitizers and annihilators contained in a liquid phase, thus the solubility of oxygen in these solvents is of much importance. **Figure 7** shows the calibration plots for the sensor SM1 obtained at 3 different temperatures. As can be seen, a pronounced decrease of the luminescence decay times can be observed when temperature is increased. In fact the decay times τ_0 were determined to be 9.0, 4.9 and 2.7 μs for the NIR phosphorescence and 276, 168 and 101 μs for the upconverted fluorescence, at 10, 25 and 40 °C, respectively. The temperature effect on the decay time of sensitizer is much higher than the thermal quenching observed for PtTPTBP in the absence of the annihilator (<0.1%/K) which can be explained by the increase in the efficiency of the triplet-triplet energy transfer. This is in good agreement with the literature data obtained for the upconvesion in rubbery polymers.[41] The sensitivity to oxygen decreases with increasing temperature for both the upconverted fluorescence and the NIR phosphorescence. Notably, the intensity of the upconverted fluorescence shows similar temperature behavior (Figure S14, Supporting Information). The Stern-Volmer constants K_{SV} calculated from the decay time plots are 7.4, 6.1 and 4.8 kPa^{-1} for the upconverted fluorescence and 0.166, 0.123 and 0.091 kPa^{-1} for the NIR phosphorescence at 10, 25 and 40 °C, respectively. The calculation of the bimolecular rate constants $k_q = K_{SV}/\tau_0$ reveals that they increase with temperature both in case of the NIR phosphorescence (18.4, 25.1 and 33.7 $Pa^{-1}s^{-1}$ at 10, 25 and 40 °C, respectively) and upconverted fluorescence (26.8, 36.4 and 47.3 $Pa^{-1}s^{-1}$ for the same temperatures).

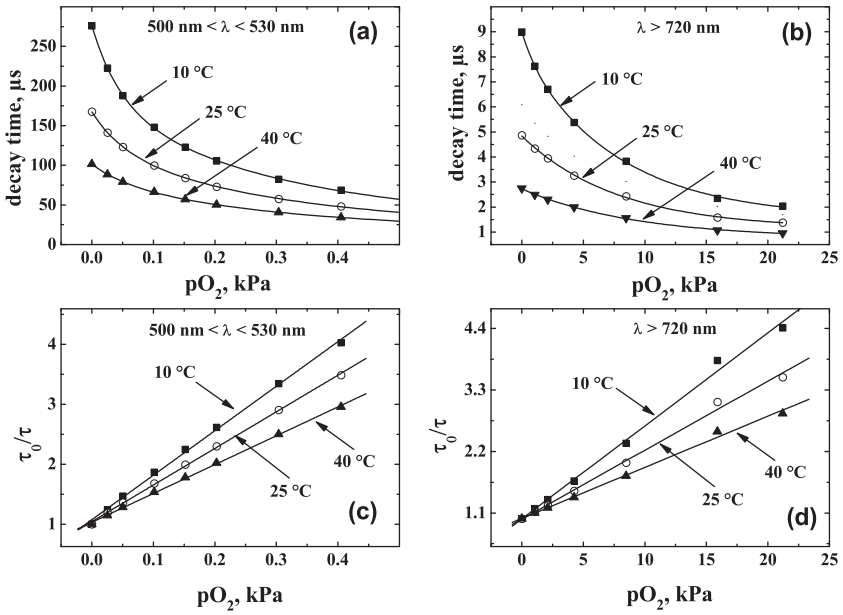

Figure 7. Decay times (a,b) and Stern-Volmer plots (c,d) obtained for SM1 at different temperatures. Excitation was performed with a 605 nm LED. For (a,c) the emission was isolated with a 515/30 band-pass filter and a modulation frequency of 555 Hz was used; for (b,d) the NIR-phosphorescence was isolated with an RG-9 filter and a modulation frequency of 30 kHz was used.

2.9. Response Times and Operational Stability

Figure 8a shows the dynamic response of the SM1 to 0.101 kPa of oxygen. As can be seen, the response of the sensor is fairly fast despite the relatively thick layer (about 50 µm, which includes the sensing and the light reflecting layers). The response times t_{95} (defined as the time needed for the sensor signal to change to 95% of the original value) were estimated to be 18 s when sharply increasing the pO_2 from 0 kPa to 0.1 kPa and 40 s for the reverse process. Figure 8b demonstrates that the sensor responds fully reversibly to altering pO_2. It should be noted that the measurements were performed each 45 s to avoid photobleaching.

2.10. Photostability

Photostability is an important parameter if practical applications of the optical sensor are considered. Literature reports on the photostability of the TTA upconversion systems are rare. Notably, most systems were investigated in deoxygenated solutions and relatively slow photodegradation can be difficult to detect because the photodegradation products are distributed in the whole volume of a cuvette. Nevertheless, Singh-Rachford and Castellano reported noticeable photodegradation of rubrene in a TTA-based upconversion system which was attributed to the formation of non-fluorescent rubrene-endoperoxide due to oxidation by singlet oxygen.[22] On the other hand, perylene dyes are generally considered as highly photostable.[45] In case of the new sensing materials virtually no photobleaching is noticeable in the absence of oxygen (Figure S15, Supporting Information) under continuous excitation with the red light (240 µmol s^{-1} m^{-2}). However, the upconverted fluorescence decreases rather fast if oxygen is introduced. This is accompanied by an increase in the NIR phosphorescence of PtTPTBP which clearly indicates lower efficiency of the T-T energy transfer. Thus, oxidation of the perylene dye with photosensitized singlet oxygen (produced either by the perylene itself or by the Pt(II) porphyrin) is the most likely photodegradation passway. Both, the ground state and the triplet excited state of the perylene, can be involved in oxidation but the second possibility seems to be more likely due to the higher reactivity of the excited molecules in red-ox reactions. Clearly, such fast photobleaching can not be observed in a typical experiment where a perylene dye is excited directly since no population of the triplet state occurs and formation of singlet oxygen is marginal. It can be concluded here that improvement of the photostability is necessary to enable prolong measurements with TTA upconversion-based oxygen sensors without recalibration. Annihilators such as anthracene derivatives or even other perylene dyes may have substantially different reactivity towards singlet oxygen and be more promising for designing highly photostable anti-Stokes oxygen sensors.

3. Conclusions

It was possible to demonstrate a novel type of an optical oxygen sensor by employing triplet-triplet annihilation-based upconversion and realising a solid state sensor. Oxygen-sensitive anti-Stokes fluorescence is clearly the main feature of the sensor. New material enables interrogation via ratiometric measurements of the luminescence intensities (upconveted fluorescence/NIR phosphorescence) and the measurement of the luminescence decay times of both components. Notably, the measurement of the decay times is preferable since the intensity-based calibration plots are dependent on the intensity of the excitation light. In contrast to conventional optical sensors, the new material enables monitoring of oxygen in a very broad dynamic range (from ultratrace amounts to pO_2 exceeding air saturation) due to the very different sensitivities of luminescence signals to oxygen. New sensing materials possess acceptable response times of < 1 min and good operational stability but can suffer from noticeable photodegradation under continuous irradiation in presence of oxygen. Photodegradation is attributed to oxidation of the annihilator by photosensitized singlet oxygen. The new concept can be particularly promising for applications where measurement of pO_2 in a very broad dynamic range (trace quantities–air saturation) is required and in media with high level of background fluorescence (e.g. photosynthetic systems). Considering the great amount of available sensitizers and annihilators the new sensing concept allows design of oxygen sensors with tailor-made optical properties.

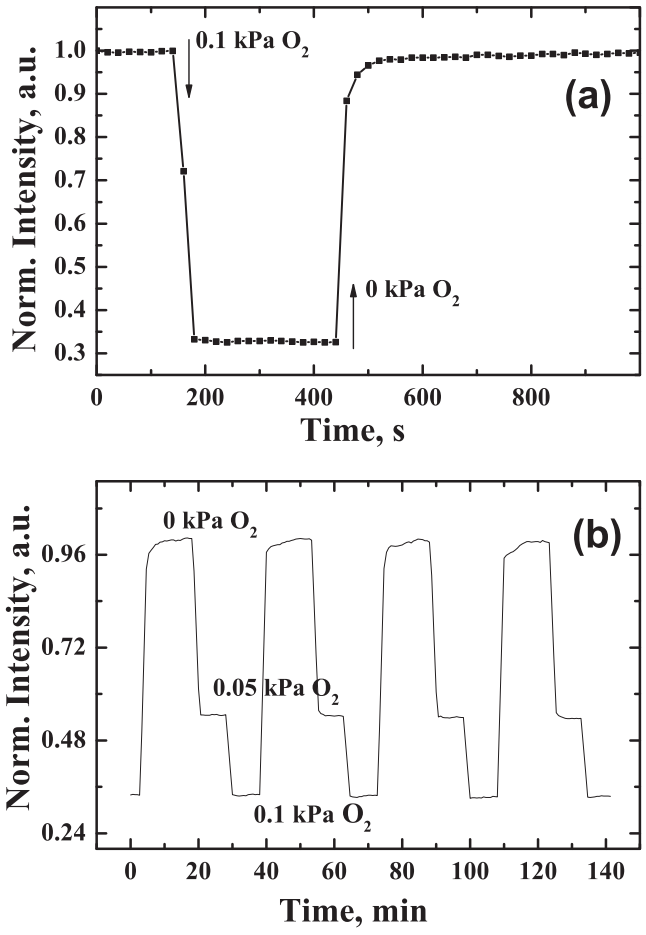

Figure 8. Dynamic response of the sensor SM1 to 0.1 kPa O_2 (a) and to variations of pO_2 (b); $\lambda_{exc} = 615$ nm, $\lambda_{em} = 505$ nm.

4. Experimental Section

Materials: Poly(propylene glycol) (PPG, MW 1.200) and n-butyl benzyl phthalate (BBP) were obtained from Aldrich (www.sigmaaldrich.com); lipophilic titanium dioxide nanoparticles (P170) was from Degussa (www.corporate.evonik.de), Teflon AF 1600–from DuPont (www.dupont.com), porous glass beads Trisopor micro ($d_{50} = 4.7$ µm, pore size 98 nm, specific surface 45.5 $m^2\ g^{-1}$)–from VitraBio GmbH (Steinach, Germany, www.vitrabio.de) and poly(ethylene glycol terephthalate) support (Mylar)–from Goodfellow (www.goodfellow.com). Vinyl-terminated polydimethylsiloxane (viscosity 1000 cSt.), methylhydrosiloxane/dimethylsiloxane copolymer (HMS-301), tetravinyltetramethyl cyclotetrasiloxane, platinum divinyltetramethyl siloxane complex, diisobutyl 3,9-perylenedicarboxylate and perfluorodecalin were purchased from ABCR (www.abcr.de). All solvents were from Roth (www.carl-roth.de). Nitrogen, synthetic air and test gas (1% oxygen in nitrogen) (all of 99.999% purity) were obtained from Air Liquide (www.airliquide.at). Preparation of Pt(II) and Pd(II) complexes with tetraphenyltetrabenzoporphyrin (PtTPTBP and PdTPTBP, respectively) is reported elsewhere.[47]

Preparation of the Oxygen-Sensitive Particles: A solution containing 1 g of a high-boiling solvent (BBP or PPG), 1 mg of a sensitizer (PtTPTBP or PdTPTBP) and 1 mg of diisobutyl 3,9-perylenedicarboxylate in 6 mL of dichloromethane was added dropwise under vigorous stirring to a suspension of 2.5 g of the porous glass beads in 15 mL of dichloromethane. The resulted suspension was stirred at room temperature until most of dichloromethane evaporated to form a powder which was dried for 30 min at 60 °C.

Preparation of the Oxygen Sensors SM1, SM2 and SM4: An agate mortar was used to disperse 600 mg of the oxygen-sensitive particles in 1 g of the vinyl-terminated polydimethylsiloxane. The viscose suspension was diluted with 1.6 g of hexane; then 40 µL of the methylhydrosiloxane/dimethylsiloxane copolymer, 3 µL of tetravinyltetramethyl cyclotetrasiloxane and finally 5 µL of the platinum divinyltetramethyl siloxane complex were added. The sensor "cocktail" was knife-coated on dust-free microscopic slides or on a Mylar support using a 75 µm spacer. After evaporation of the solvent the composition was allowed to polymerize for 1 h at r.t. A scattering layer (350 mg of titanium dioxide, 1 g of the vinyl-terminated polydimethylsiloxane, 40 µL of methylhydrosiloxane/dimethylsiloxane copolymer, 3 µL of tetravinyltetramethyl cyclotetrasiloxane and 5 µL of the platinum divinyltetramethyl siloxane complex in 1.75 g of hexane) was coated on the sensing layer using the same spacer. To complete the polymerization the sensor was kept at 60 °C for 30 min.

Preparation of the Oxygen Sensor SM3: An agate mortar was used to disperse 200 mg of the oxygen-sensitive particles in 2 g of the Teflon AF solution (5% wt. in perfluorodecalin). The sensor "cocktail" was knife-coated on dust-free microscopic slides using a 75 µm spacer to produce about 10 µm-thick sensing layers after solvent evaporation. A scattering layer (40 mg of titanium dioxide, 100 mg of Teflon AF and 1900 mg of perfluorodecalin) was added above the sensing layer using the same spacer.

Measurements: Emission spectra were acquired on a Fluorolog 3 from Horiba (www.horiba.com) equipped with a NIR-sensitive photomultiplier R2658 from Hamamatsu (www.hamamatsu.com) optimized for the spectral range of 300-1050 nm. All spectra were corrected for the sensitivity of the PMT using a correction function from the manufacturer. The oxygen sensors (on a glass support) were fixed in a home-made flow-through cell positioned at 60° with respect to the excitation light. The excitation slit of 14 nm was used to provide the maximum excitation intensity. A lens was positioned in front of the probe to focus the excitation light. The photon flux density determined with a Li-250A light meter from Li-COR (www.licor.com) was 240 µmol s^{-1} m^{-2}. A red laser diode module (LJM series, λ = 635 nm) obtained from Roithner (www.roithner-laser.com) was used as an alternative excitation source in case of the SM4 material.

The luminescence intensity decay curves were obtained in the time domain on a Fluorolog 3 using a pulse xenon lamp as the excitation source. Luminescence decay times were determined in the frequency domain using a two-phase lock-in amplifier (SR830, Stanford Research Inc., www.thinksrs.com). A bifurcated fiber bundle was used to guide the excitation light to the sensor and the emission light back to the photomultiplier (H5701-02, Hamamatsu, www.sales.hamamatsu.com). Excitation was performed with the light of a 605-nm LED (for SM1-SM3) or a 625-nm LED (for SM4), both from Roithner. The excitation light was filtered through a HC 620/52 band-pass filter (Analysentechnik, www.ahf.de). A band-pass filter HQ 515/30 (Analysentechnik) in combination with a plastic Dark Green filter from Lee Filters (www.leefilters.com) was used for the upconverted emission. A long-pass RG 9 filter (Schott, www.schott.com) was employed to isolate the NIR phosphorescence. The modulation frequencies were 555 Hz and 30 kHz for the upconverted fluorescence and the NIR phosphorescence, respectively. Temperature was controlled by a cryostat ThermoHaake DC50 (www.thermo.com). Gas calibration mixtures were obtained using gas mixing devices from MKS (www.mksinst.com) and Red-y (www.red-y.com).

The photographic images of the sensor foil were acquired with a Canon 5D digital camera. A piece of a sensing foil S4 on a Mylar support was positioned in a 1 cm glass cuvette. Deoxygenated was performed by using a solution of glucose (C = 0.25 M) and glucose oxidase (10 U/mL). Excitation was performed with a 3 W 625 nm LED from Roithner (light density about 1200 µmol s^{-1} m^{-2} photons). A Peacock Blue plastic filter from Lee Filters was used to visualize the upconverted emission.

Supporting Information

Supporting Information is available from the Wiley Online Library or from the author.

Acknowledgements

The work was supported by European Research Council (Project "Oxygen", N 207233).

Received: March 21, 2012
Revised: May 22, 2012
Published online: June 20, 2012

[1] I. Sánchez-Barragán, J. M. Costa-Fernández, A. Sanz-Medel, M. Valledor, J. C. Campo, *Trends Anal. Chem.* **2006**, *25*, 958.
[2] S. M. Grist, L. Chrostowski, K. C. Cheung, *Sensors* **2010**, *10*, 9286.
[3] Y. Amao, I. Okura, *J. Porphyrins Phthalocyanines* **2009**, *13*, 1111.
[4] X. Wang, H. Chen, Y. Zhao, X. Chen, X. Wang, X. Chen, *Trends Anal. Chem.* **2010**, *29*, 319.
[5] S. M. Borisov, I. Klimant, *Anal. Chem.* **2007**, *79*, 7501.
[6] S. Borisov, G. Zenkl, I. Klimant, *ACS Appl. Mater. Interfaces* **2010**, *2*, 366.
[7] D. B. Papkovsky, G. V. Ponomarev, W. Trettnak, P. O'Leary, *Anal. Chem.* **1995**, *67*, 4112.
[8] G. Khalil, M. Gouterman, S. Ching, C. Costin, L. Coyle, S. Gouin, E. Green, M. Sadilek, R. Wan, J. Yearyean, B. Zelelow, *Porphyrins Phthalocyanines* **2002**, *6*, 135.
[9] O. S. Finikova, A. V. Cheprakov, I. P. Beletskaya, P. J. Carroll, S. A. Vinogradov, *J. Org. Chem.* **2004**, *69*, 522.
[10] O. S. Finikova, S. E. Aleshchenkov, R. P. Briñas, A. V. Cheprakov, P. J. Carroll, S. A. Vinogradov, *J. Org. Chem.* **2005**, *70*, 4617.
[11] S. M. Borisov, G. Nuss, I. Klimant, *Anal. Chem.* **2008**, *80*, 9435.
[12] M. A. Yaseen, V. J. Srinivasan, S. Sakadži , W. Wu, S. Ruvinskaya, S. A. Vinogradov, D. A. Boas, *Opt. Express* **2009**, *17*, 22341.
[13] A. Y. Lebedev, A. V. Cheprakov, S. Sakadzic, D. A. Boas, D. F. Wilson, S. A. Vinogradov, *ACS Appl. Mater. Interfaces* **2009**, *1*, 1292.
[14] T. V. Esipova, A. Karagodov, J. Miller, D. F. Wilson, T. M. Busch, S. A. Vinogradov, *Anal. Chem.* **2011**, *83*, 8756.
[15] O. S. Finikova, A. Y. Lebedev, A. Aprelev, T. Troxler, F. Gao, C. Garnacho, S. Muro, R. M. Hochstrasser, S. A. Vinogradov, *Chem. Phys. Chem.* **2008**, *9*, **1673**.
[16] S. Sakadzic, E. Roussakis, M. A. Yaseen, E. T. Mandeville, V. J. Srinivasan, K. Arai, S. Ruvinskaya, A. Devor, E. H. Lo, S. A. Vinogradov, D. A. Boas, *Nat. Methods* **2010**, *7*, 755.
[17] J. Lecoq, A. Parpaleix, E. Roussakis, M. Ducros, Y. G. Houssen, S. A. Vinogradov, S. Charpak, *Nat. Med.* **2011**, *17*, 893.
[18] D. E. Achatz, R. J. Meier, L. H. Fischer, O. S. Wolfbeis, *Angew. Chem. Int. Ed.* **2011**, *50*, 260.
[19] L.-N. Sun, H. Peng, M. I. J. Stich, D. Achatz, O. S. Wolfbeis, *Chem. Commun.* **2009**, 5000.
[20] R. Ali, S. M. Saleh, R. J. Meier, H. A. Azab, I. I. Abdelgawad, O. S. Wolfbeis, *Sens. Actuators B* **2010**, *150*, 126.
[21] H. S. Mader, O. S. Wolfbeis, *Anal. Chem.* **2010**, *82*, 5002.
[22] T. N. Singh-Rachford, F. N. Castellano, *J. Phys. Chem. A* **2008**, *112*, 3550.
[23] T. N. Singh-Rachford, A. Haefele, R. Ziessel, F. N. Castellano, *J. Am. Chem. Soc.* **2008**, *130*, 16164.
[24] S. Ji, W. Wu, W. Wu, H. Guo, J. Zhao, *Angew. Chem. Int. Ed.* **2011**, *50*, **1626**.
[25] W. Wu, W. Wu, S. Ji, H. Guo, J. Zhao, *Dalton Trans.* **2011**, *40*, 5953.
[26] J. Sun, W. Wu, H. Guo, J. Zhao, *Eur. J. Inorg. Chem.* **2011**, *2011*, 3165.
[27] J. Zhao, S. Ji, H. Guo, *RSC Adv.* **2011**, *1*, 937.
[28] T. N. Singh-Rachford, F. N. Castellano, *J. Phys. Chem. Lett.* **2010**, *1*, 195.
[29] T. N. Singh-Rachford, F. N. Castellano, *Coord. Chem. Rev.* **2010**, *254*, 2560.
[30] R. R. Islangulov, D. V. Kozlov, F. N. Castellano, *Chem. Commun.* **2005**, 3776.
[31] W. Wu, H. Guo, W. Wu, S. Ji, J. Zhao, *J. Inorg. Chem.* **2011**, *50*, 11446.
[32] A. Turshatov, D. Busko, S. Baluschev, T. Miteva, K. Landfester, *New J. Phys.* **2011**, *13*, 083035.
[33] W. Wu, J. Sun, S. Ji, W. Wu, J. Zhao, H. Guo, *Dalton Trans.* **2011**, *40*, 11550.
[34] W. Wu, H. Guo, W. Wu, S. Ji, J. Zhao, *J. Org. Chem.* **2011**, *76*, 7056.
[35] S. Ji, H. Guo, W. Wu, W. Wu, J. Zhao, *Angew. Chem. Int. Ed.* **2011**, *50*, 8283.
[36] C. Wohnhaas, A. Turshatov, V. Mailänder, S. Lorenz, S. Baluschev, T. Miteva, K. Landfester, *Macromol. Biosci.* **2011**, *11*, 772.
[37] P. B. Merkel, J. P. Dinnocenzo, *J. Luminesc.* **2009**, *129*, 303.
[38] A. Monguzzi, R. Tubino, F. Meinardi, *J. Phys. Chem. A* **2009**, *113*, 1171.
[39] A. Monguzzi, M. Frigoli, C. Larpent, R. Tubino, F. Meinardi, *Adv. Funct. Mater.* **2012**, *22*, 139.
[40] R. R. Islangulov, J. Lott, C. Weder, F. N. Castellano, *J. Am. Chem. Soc.* **2007**, *129*, 12652.
[41] T. N. Singh-Rachford, J. Lott, C. Weder, F. N. Castellano, *J. Am. Chem. Soc.* **2009**, *131*, 12007.
[42] S. Ji, W. Wu, W. Wu, H. Guo, J. Zhao, *Angew. Chem. Int. Ed.* **2011**, *50*, 1626.
[43] Y. Y. Cheng, T. Khoury, R. G. C. R. Clady, M. J. Y. Tayebjee, N. J. Ekins-Daukes, M. J. Crossley, T. W. Schmidt, *Phys. Chem. Chem. Phys.* **2009**, *12*, 66.
[44] T. N. Singh-Rachford, A. Nayak, M. L. Muro-Small, S. Goeb, M. J. Therien, F. N. Castellano, *J. Am. Chem. Soc.* **2010**, *132*, 14203.
[45] G. Seybold, G. Wagenblast, *Dyes Pigm.* **1989**, *11*, 303.
[46] Z. Zhou, R. Shinar, A. J. Allison, J. Shinar, *Adv. Funct. Mater.* **2007**, *17*, 3530.
[47] S. M. Borisov, G. Nuss, W. Haas, R. Saf, M. Schmuck, I. Klimant, *J. Photochem. Photobiol. A.* **2009**, *201*, 128.
[48] S. M. Borisov, P. Lehner, I. Klimant, *Anal. Chim.* **2011**, *690*, 108.